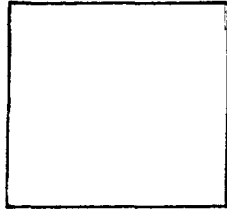


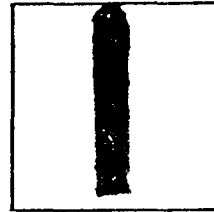
PHOTOGRAPH THIS SHEET

ADA 079929

DTIC ACCESSION NUMBER



LEVEL



INVENTORY

FTD-ID(RS)T-0730-79

DOCUMENT IDENTIFICATION

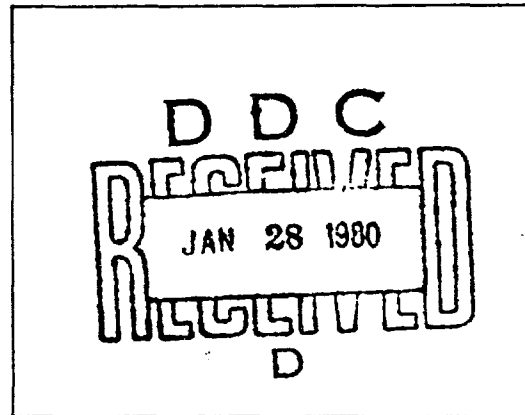
DISTRIBUTION STATEMENT A

Approved for public release;
Distribution Unlimited

DISTRIBUTION STATEMENT

ACCESSION FOR	
NTIS	GRA&I <input checked="" type="checkbox"/>
DTIC	TAB <input type="checkbox"/>
UNANNOUNCED	<input type="checkbox"/>
JUSTIFICATION	
BY	
DISTRIBUTION /	
AVAILABILITY CODES	
DIST	AVAIL AND/OR SPECIAL
A	

DISTRIBUTION STAMP



DATE ACCESSIONED

79 11 13 256

DATE RECEIVED IN DTIC

PHOTOGRAPH THIS SHEET AND RETURN TO DTIC-DDA-2

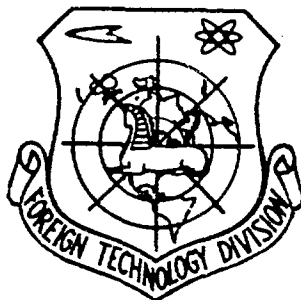
FOREIGN TECHNOLOGY DIVISION



COMPARISON OF THE AERODYNAMIC PROPERTIES OF
AIRCRAFT WITH A CANARD AND A
CONVENTIONAL ARRANGEMENT

by

Jan Staszek



Approved for public release;
distribution unlimited.

ADA 079929



EDITED TRANSLATION

FTD-ID(RS)T-0730-79

13 June 1979

MICROFICHE NR: *FTD-79-C-000774*COMPARISON OF THE AERODYNAMIC PROPERTIES OF
AIRCRAFT WITH A CANARD AND A CONVENTIONAL
ARRANGEMENT

By: Jan Staszek

English pages: 22

Source: Prace Instytutu Lotnictwa, Nr. 63, 1975,
pp. 63-78.

Country of origin: Poland

Translated by: LINGUISTIC SYSTEMS, INC.
F33657-78-D-0618
Thaddeus Szkoda

Requester: FTD/TQTA

Approved for public release; distribution
unlimited.

THIS TRANSLATION IS A RENDITION OF THE ORIGINAL FOREIGN TEXT WITHOUT ANY ANALYTICAL OR EDITORIAL COMMENT. STATEMENTS OR THEORIES ADVOCATED OR IMPLIED ARE THOSE OF THE SOURCE AND DO NOT NECESSARILY REFLECT THE POSITION OR OPINION OF THE FOREIGN TECHNOLOGY DIVISION.

PREPARED BY:

TRANSLATION DIVISION
FOREIGN TECHNOLOGY DIVISION
WP-AFB, OHIO.

FTD -ID(RS)T-0730-79

Date 13 June 19 79

Comparison of the aerodynamic properties of aircraft with a Canard and a Conventional arrangement by Jan Staszek

Summary

An attempt is made to represent in a quantitative manner the advantages and the drawbacks of a Canard Airplane to be taken into consideration during the early design work. The range of the lift and drag coefficient of the wing alone and the wing with the control surfaces are determined for the canard airplane and compared with those for the conventional system. The action of the air stream leaving the elevator and flowing towards the main wing is discussed as well as methods for reducing the influence of downwash by means of:

- application of a twisted wing to achieve the required angle of incidence
- correct selection of control surface setting
- correct selection of aspect ratio for the control surfaces
- correct location of the wing with respect to the control surfaces.

As a result of the analysis it is found that the canard system has, under some conditions, properties approaching those of the conventional system and that it is, for some configurations, more advantageous as regards the possibility of obtaining maximum lift.

- b -span
- Cx'_s -wing drag coefficient
- Cx_u -control surface drag coefficient
- Cz'_s -coefficient of aerodynamic lift for wing
- Cz_u -coefficient of aerodynamic lift for control surface
- Cz'_s -coefficient of aerodynamic lift for wing in deflected flow
- Cx'_s -coefficient of drag for wing in deflected flow
- c_s -mean chord of wing
- c_u -mean chord of control surface
- e -distance past trailing edge where horseshoe vortex is fully formed
- K -Kaden constant
- r_r -radius of the vortex core
- S_s -wing area
- S_w -control surface area
- V -velocity
- α -angle of attack of the wing
- β -angle of setting for the control surface
- ϵ -stream deflection angle
- λ -aspect ratio
- $\sigma = \frac{S_w}{S_s}$ -relationship of control surface area to wing area

1. Introduction

A quantitative determination of the effect of deflected air flow from a control surface to the main wing is of the utmost importance in definite solutions to canard arrangements. Also of interest is the comparison of aerodynamic properties of this arrangement with the generally employed conventional arrangement.

Despite the lack of data in literature pertaining to the effect of aspect ratio and magnitude of angle setting for canard control surfaces as well as the magnitude of wing twisting and vertical wing location for the arrangement's aerodynamic characteristics, based on the variation of the above named parameters, a curve analysis was carried out. In the process of this analysis, an approximate method was applied taking partial advantage of wind tunnel data.

2. Stream deflection of a canard control surface

As an effect of the disturbed flow caused by a control surface the angle through which air flows around individual parts of the wing of a canard changes along the span. A precise determination of the velocity distribution in the space after the canard control surface is very difficult because the vortex layer flowing off the control surface is not completely coiled near the wing whereas the horseshoe vortex is just in the formation stage. The distance past an airfoil where the horseshoe vortex can be considered completely formed was determined by Kaden¹ and is expressed by the formula

$$e = K \frac{\lambda^2}{C_z} c \quad (1)$$

for which K equals 0.28 for an elliptical force distribution along the span. This formula, for a control surface with an aspect ratio λ_w equal to 5, expresses this distance as $e = 7 \frac{c_u}{C_z}$

Taking into consideration that the wing is located at an almost even distance of $4c_u$, it is maintained that the vortex layer is completely coiled and the horseshoe vortex completely formed only when $4c_u = 7 \frac{c_u}{C_z}$ for which $C_z \cong 1.75$. This indicates that when C_z is less than 1.75, the flow after the control surface at the wing location is still in the formation stage and the velocity distribution along with the associated distribution of stream deflection angles is very difficult to determine theoretically.

Taking the above into account, an experimentally selected distribution of vertical velocity components of streams past the cont-

rol surface was introduced into the analysis, describing the stream deflection angles within the boundaries of the control surface span b_u .² A hyperbolic velocity distribution was established for the wing exterior (past the range of control surface span) given by the equation $vr = \text{const}$ taking as a basis velocities selected experimentally for internal parts of the vortex core.

Figure 1 shows the canard arrangement accepted for analysis while the vertical distance of the airfoil from the horizontal plane passing through the aerodynamic axis of the control surface is illustrated in Figure 4.

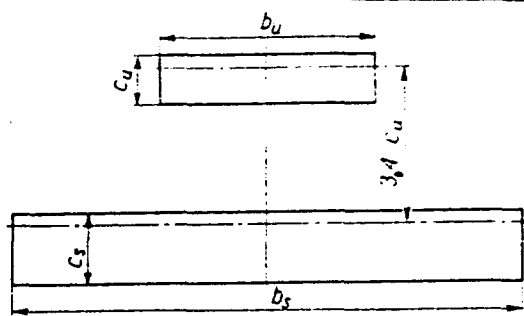


Figure 1. Canard arrangement chosen for analysis where $\lambda = 7$, $\lambda_u = 5$, $\sigma = \frac{S_s}{S_1} = 0.3$

In practice, a canard control surface is usually placed somewhat further from the wing than shown in Fig. 1. Experimental data for the distribution of vertical velocities past the control surface are unavailable with the exception of Report number 651 NACA². These data include vertical velocity distribution (stream deflection angle) only for distances of $1.3c_u$ and $3.4c_u$ after the control surface. Flow in this region is yet unformed and its theoretical description is difficult. Despite this, for further considerations a vertical velocity distribution for a distance of $3.4c_u$ after the control surface was used, in agreement with the above referenced NACA wind tests, although in actuality this distribution will obviously differ for each different angle of attack or distance past the control surface. The difference should not be that great though this is a postulation not supported by experimental data.

A second simplification in these considerations is the disregard for the airstream deflection at the location of the control

surface caused by the influence of the wing on the flow just before it. A realistic angle of attack for the control surface is for this reason somewhat larger depending on the C_z of the wing. In this case the difference is not large and can be neglected.

Figure 2 shows the formation and orientation of the horseshoe vortex axis in accordance to the NACA² measurements whereas Figure 3 shows a graph of measured stream deflection angles along the intersection line of the vertical plane which contains the aerodynamic axis of the wing with the horizontal planes whose vertical distances from the aerodynamic axis of the control surface are given in units of the control surface span b_u^2 .

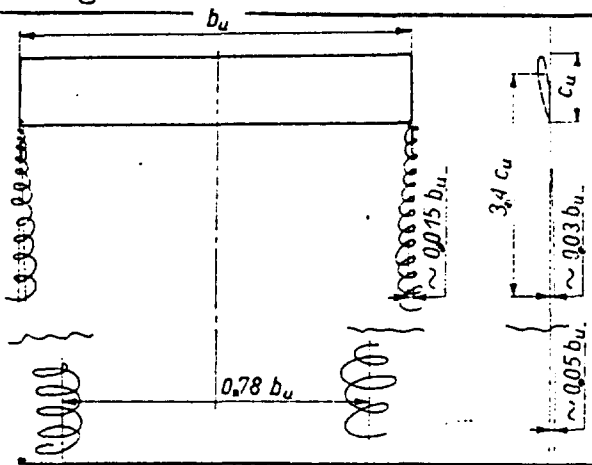


Figure 2. Position of the horseshoe vortex at $3.4c_u$ and at a large distance

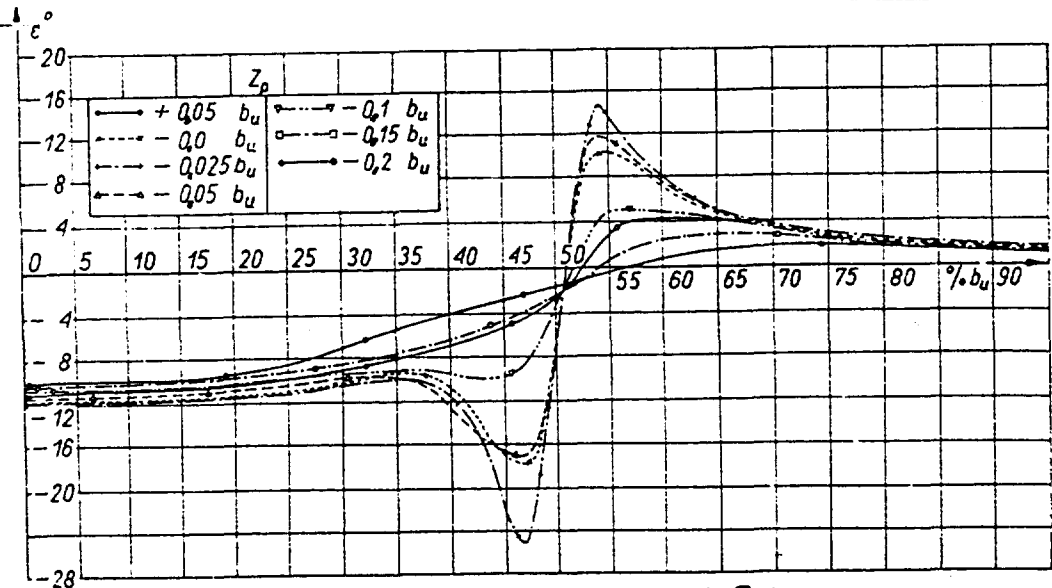


Figure 3. Stream deflection angles along the wing span at a distance of 3.4 times the mean chord of the control surface where

C_z equals 1.35, b_u is the control surface span, λ_u is the aspect ratio of the control surface, Z_p is the distance from the horizontal plane to the aerodynamic axis of the wing.

Figure 4 shows the geometric construction making possible the description of vertical components of flow velocity from the given velocity distribution of Rankine's vortex whose axis as well as core diameter are taken from NACA measurements. The location of the vortex axis is shown in Fig. 2 and 3 given that its core radius at this location is about 3.4 percent of b_u while its axis lies at a distance of about 3 percent b_u below the horizontal plane containing the aerodynamic axis of the control surface.

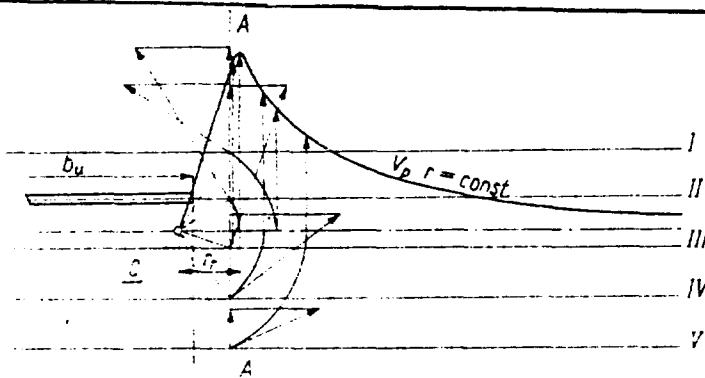


Figure 4. Assignment of the distribution of vertical velocity components on the exterior of the control surface span:

A-A is the plane in which vertical components V are

measured, r_r is the vortex core radius, I is the distance of $0.05 b_u$ above the aerodynamic axis of the control surface, II is the level of the control surface aerodynamic axis, III is the level $0.05 b_u$ below the control surface aerodynamic axis, IV is the level $0.1 b_u$ below the control surface aerodynamic axis, V is the level $0.15 b_u$ below the control surface aerodynamic axis, O is the axis of free vortex.

The axis of the horseshoe vortex is often parallel to the direction of undisturbed flow and does not shift in the vertical direction at the rate it is displaced to the end. Both vortex branches converge in a vertical plane to asymptotes separated by a distance of $0.78 b_u$ at a sufficiently large distance past the control surface.

For the distance in question, at the location of the main wing, the displacement of the vortex axis from the end of the control surface span to its center does not exceed 1.5 percent b_u (distance between vortices is about $0.97 b_u$).

The stream deflection angle in the system's plane of symmetry is given by the formula $\varepsilon = \frac{46.2}{\lambda_u} C_{z_u}$ (2) and does not change much for a range around $0.7 b_u$.

The stream deflection past the control surface causes the entire part of the wing located between the horseshoe vortex axes originating from the control surface to have a smaller increment $\frac{\Delta C_{z_1}}{\Delta \alpha}$, although the actual angle of attack α_n is expressed as $\alpha_n = \alpha - \varepsilon$ (3) while its increment is $\Delta \alpha_n = \Delta \alpha - \Delta \varepsilon$ (3a).

Equation (2) indicates that by decreasing the control surface aspect ratio, it is possible to create a very disadvantageous situation for the part of the wing lying in the zone of separated streams leaving the stabilizer between the horseshoe vortex axes. Alternatively, in the case when increasing the angle of attack by $\Delta \alpha$ causes a simultaneous increase in the stream deflection angle $\Delta \varepsilon$ thereby balancing each other out. This indicates that the part of the wing lying in a zone between the horseshoe vortex axes caused by the control surface does not undergo an increment in angle of attack in relation to stream flowing from the control surface. In other words, $\frac{\partial C_{z_1}}{\partial \alpha}$ for this part of the wing is then either zero or close to it. This instance occurs when $\lambda_u \cong 2.5$ and $\lambda_s \cong 6$. Upon further decrease of λ_u , the differential $\frac{\partial C_{z_1}}{\partial \alpha}$ assumes negative values.

Outside the horseshoe vortex axis the situation is reversed and the increment $\frac{\Delta C_{z_1}}{\Delta \alpha}$ is larger than for a wing without a control surface since the actual angle of attack is $\alpha_n = \alpha + \varepsilon$ (4) and its increment $\alpha_n = \Delta \alpha + \Delta \varepsilon$ (4a).

In this case, the stream deflection angle changes along the wing span in accordance ^{with} the distribution of velocity originating from the free vortex though in contrast to the previous example where the angle was almost constant in the central area of the horseshoe vortex.

The increment $\frac{\Delta C_{z_s}}{\Delta \alpha}$ for that part of the wing located outside the vortex axis is larger only within a certain range of angles of attack α , and also when the actual angle of attack α_n approaches a value at which C_{z_s} attains a maximum. Exceeding this value by α_n produces a negative increment $\frac{\Delta C_{z_s}}{\Delta \alpha}$ while the central part of the wing will have a positive $\frac{\Delta C_{z_s}}{\Delta \alpha}$. This indicates that a canard control surface accelerates flow separation at the ends of the main wing.

The above leads to the conclusion that the main wing of a canard lying in a stream with interference from a frontal control surface does not attain a value of $C_{z_s, \max}$ as would a wing in undisturbed flow.

The situation is similar for drag coefficient C_{x_s} for the wing of a canard. Figure 5a shows a distribution of forces acting on an element of the wing between the horseshoe vortex axes, caused by a frontal control surface.

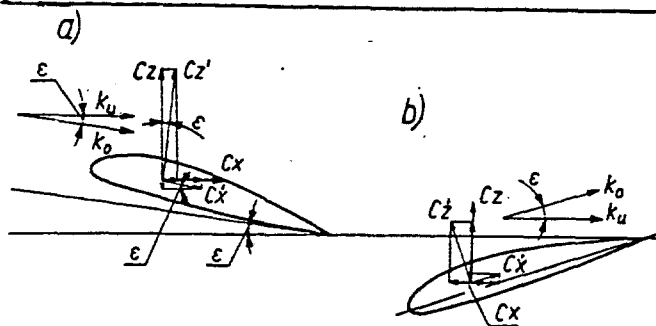


Figure 5. Coefficients C_z and C_x for a canard wing element referenced to the direction of undisturbed flow for a) interior b) exterior part of the horseshoe vortex, k_u is the direction of undisturbed flow, k_0 is the direction of deflected flow.

This arrangement leads to the result that in the range of angles of attack in normal flight, the coefficient of lift C_{z_s}

of a wing element is always smaller than in the case of flow undisturbed by a control surface. The coefficient of lift Cx_s of this element, however, will always be larger than in the case with undisturbed flow. These coefficients calculated for undisturbed flow direction are expressed by the following formulae:

$$Cz = Cz' \cos \varepsilon - Cx' \sin \varepsilon \quad (5) \quad Cx = Cx' \cos \varepsilon + Cz' \sin \varepsilon \quad (5a)$$

Obviously, along with the increase in the angle of attack and stream deflection angle ε , the drag coefficient Cx_s for a central wing element will grow faster for a wing in a canard arrangement than a drag coefficient Cx_s for a wing in a conventional arrangement where this element is subject to undisturbed flow.

Figure 5b shows the distribution of forces acting on a wing element located outside the horseshoe vortex axis, caused by a frontal control surface. Despite the stream deflection angle ε being positive here, a greater value of lift coefficient Cz_s is attained than in the case of undisturbed flow. This increase is caused by the sum of the projections Cz' and Cx' on the direction perpendicular to the direction of undisturbed flow. In describing the drag coefficient Cx_s , projections Cx' and Cz' on a direction parallel to the direction of undisturbed flow are subtracted thus;

$$Cz = Cz' \cos \varepsilon + Cx' \sin \varepsilon \quad (6) \quad Cx = Cx' \cos \varepsilon - Cz' \sin \varepsilon \quad (6a)$$

The result of such an arrangement of aerodynamic forces acting on a wing element located outside the horseshoe vortex axis is that within the range of small angles of attack α , the drag coefficient Cx of this element in a direction parallel to undisturbed flow may be smaller for a canard arrangement than for a conventional one, and can even accept negative values in certain cases.

3. Properties of an untwisted wing of a canard

For a quantitative description of the influence of stream

deflection past a control surface on wing characteristics, lift and drag coefficients, Cz_s , Cx_s of an untwisted wing were calculated taking into account the stream deflection range given in Figure 3. A canard arrangement was taken as shown in Figure 1 assuming a I.A. 608 wing profile with an aspect ratio of λ_s equal to 7 and the same profile for the control surface with an aspect ratio λ_c equal to 5. The relation of control surface area to wing area was set at σ equal to 0.3 with the assumption that the wing is located in a plane a distance $0.075 b_u$ below the plane of the control surface. The angle of setting for the control surface was taken as β equal to 2.5 degrees.

Figure 6 shows a graph of a simplified distribution of stream deflection angles along the wing span. Stream deflection angles in the plane of symmetry were calculated according to equation (2) while stream deflection angles ϵ for individual wing elements were taken from Figure 3 using in the calculations the stream deflection angle in the plane of symmetry of the arrangement as a comparative angle.

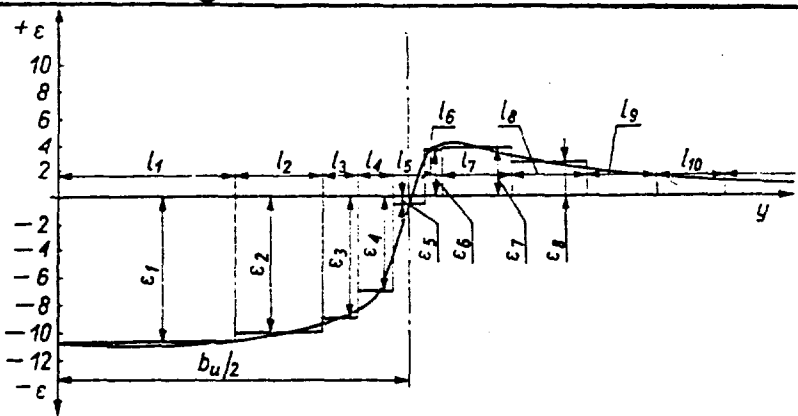


Figure 6. Simplified graph of stream deflection angles along the wing span at the distance of $3.4 c_u$ past the aerodynamic axis of the control surface and $0.075 b_u$ beneath the axis, for

a_1	a_2	a_3	a_4	a_5	a_6	a_7	a_8	a_9	a_{10}	
.5	.25	.1	.1	.1	.05	.2	.2	.2	.2	$a_n = 2l_n/b_n, \epsilon_n = \epsilon_1 w_p$

ϵ_n is the stream deflection angle at a specific location (from the range given in Fig. 3), w_p is the coefficient dependent on wing orientation as the angle of attack changes (taken from the range in Fig. 3).

Coefficients C_x and C_z for particular wing elements were calculated according to equations (5), (5a) and (6), (6a) while actual angles of attack of these elements were delineated according to equations (3), (3a) and (4), (4a).

The results of calculations are presented in the form of graphs for curves of an untwisted wing in Figure 8 which also shows for comparison a graph for the same airfoil in a stream undisturbed by a frontal control surface.

From the comparison presented, it is observed that the influence of stream deflection is quite large and is particularly noticeable with large angles of attack when a significant increase in drag coefficient C_x along with a decrease in lift coefficient C_z is noted with the flattening of the wing curve. With smaller angles of attack, a smaller drag coefficient C_x is attained than for a wing where the flow is undisturbed by a control surface. Besides other basic principles applied to the canard arrangement, this fact demonstrates that mounting a control surface forward of the main wing may be advantageous for aircraft flying at high speeds hence small angles of attack. This phenomenon explains the existence of a correspondingly large local lift coefficients C_z' for wing elements lying outside the horseshoe vortex. This coefficient (C_z') effects the decrease of the local drag coefficient C_x' as may be surmised from equation (6a).

The acquired result is not encouraging since the expectation of an increase in lift coefficient C_z for the whole arrangement is reduced by a negative interaction of stream deflected by a control surface onto the main wing. This result leads to a search for some helpful medium for at least a partial elimination of disadvantageous effects which a frontal control surface has on a wing.

As can be seen from Fig. 3, the largest stream deflection past the control surface occurs near the axis of the horseshoe vortex.

If the wing is located at a distance greater than $1.8 r_v$ above or below the vortex axis, then the whole range of large gradients of stream deflection angles ϵ is displaced past the wing and the deterioration of the canard's aerodynamic properties is correspondingly smaller. From this deduction it is seen that wing positions II and III in Fig. 4 and Fig. 7 are disadvantageous since during flight through usable angles of attack, the core of the vortex flowing from the control surface is directed onto the main wing causing the greatest negative effects and stream deflection angles discussed above.

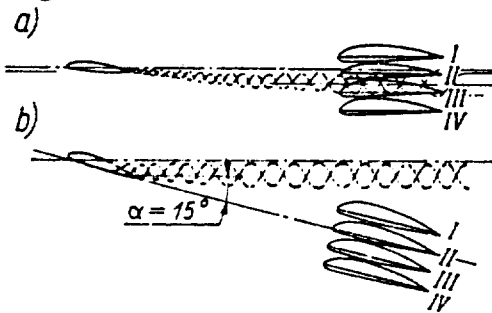


Figure 7. Vortex locations for changes in angles of attack for a canard.

Although the axis of the horseshoe vortex does not change in relation to the direction of undisturbed flow, position I in Fig. 7 above the vortex core is only apparently good since during an increase in the aircraft's angle of attack the vortex core intercepts the main wing causing an undesirable increase in stream deflection. In fact, for angles of attack on the order of $\alpha = 15^\circ$ degrees, the vortex core will be located above the main wing but for intermediate angles the wing will be under the direct influence of the vortex core.

The most advantageous wing location is position IV since the vortex core is always located past the wing and moving further away from it with a corresponding increase in the angle of attack. Taking into account the above conditions, all calculations for the canard arrangement were performed with the intent that the wing would basically be located in position IV. At the same time this would describe the canard arrangement as a low wing with the frontal control surface mounted relatively high.

4. Properties of a twisted wing of a canard

The most effective method of correcting aerodynamic properties of a wing is by twisting it geometrically such that the actual angles of attack for the elements of the airfoil in deflected flow produce an advantageous distribution of upthrust along the wing span (close to elliptical). It is thus necessary to calculate the stream deflection angle ϵ past the control surface for each element of the wing and, furthermore, setting each element under the corresponding stream deflection angle. Although the stream deflection angle ϵ as given in equation (2) is proportional to the lift coefficient for the control surface (Cz_u), the twisting of the wing can only respond to one angle of attack. This preferred angle of attack α_0 should be described in the preliminary aerodynamic analysis of aircraft taking into consideration their purpose and governing conditions of flight.

For a quantitative description of the effect of twisting the airfoil, calculations of lift and drag coefficients for a canard arrangement were presented in Fig. 1, the twisting being effected in accordance with the graph presented in Fig. 6. Profiles and surface areas of the canard arrangement under consideration were taken to be the same as in the case of the untwisted wing, and the control surface setting was similarly taken as β equal to 2.5 degrees.

The twisting was calculated for the preferred angle of attack for the wing, α_0 equal to 2.5 degrees, for Cz equal to 0.7 while curves were obtained using equations (5), (5a) and (6), (6a) for each element of the wing and summing the results for individual angles of attack. As a result, a curve for a twisted wing in a canard arrangement was obtained which was characterized by a coefficient Cx_{min} larger by about 40 percent and a coefficient Cz_{max} higher by about 6 percent than in the case of an untwisted wing. The curves obtained are shown in Figure 8.

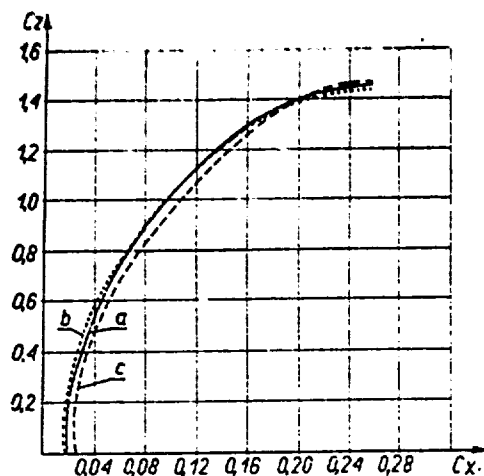


Figure 8. Comparison of wing curves in undisturbed flow for $\sigma = 0.3, \beta = 2.5^\circ, \lambda_u = 5, \lambda_s = 7$: a-wing in undisturbed flow, b-untwisted wing of a canard, c-twisted wing of a canard with $\alpha_0 = 2.5^\circ$.

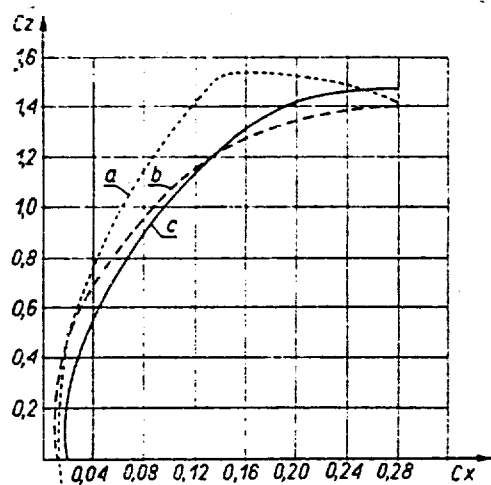


Figure 9. The influence of the choice of preferred angle α_0 and control surface setting angle β on the characteristics of the wing curve; a-comparative wing with $\alpha_0 = 2.5^\circ, \beta = 2.5^\circ, \sigma = 0.3, \lambda_u = 5$, b - twisted wing with $\alpha_0 = 0^\circ, \beta = 2.5^\circ, \sigma = 0.3, \lambda_u = 5$, c - twisted wing with $\beta = 5^\circ, \alpha_0 = 2.5^\circ, \sigma = 0.3, \lambda_u = 5$.

Decreasing the preferred angle α_0 results, in fact, in a decrease in Cx_{\min} but equally effects a decrease in Cz_{\max} forcing the wing curve to a shape it accepts for an untwisted orientation. The nature of these changes is shown in Figure 9.

Increasing the control surface setting angle β results in increasing stream deflection angle ϵ thus increasing the effect of stream deflection. Cz_{\max} then decreases while Cx_{\min} diminishes equally. The nature of these changes is shown in Figure 9.

As was foreseen, decreasing the control surface area causes a decrease on its effect on the wing whose curve distinctly improves as can be seen in Fig. 10. Moving the wing below the vortex core also has an added effect as the flow interference and stream deflection angles ϵ are smaller. For example; wing curves with

α equal to zero in the axis of free vortex as well wing curves moved downward $0.05b_u$ were recalculated. Results are shown in Figure 10.

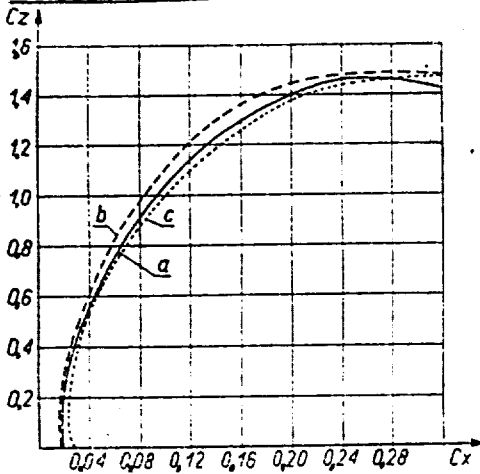


Figure 10. Effect of control surface size and wing location in a canard on curve characteristics of wing; a-comparative wing located $0.05b_u$ below vortex axis with $\sigma=0.3$, $\alpha_0=2.5^\circ$; $\beta=2.5^\circ$, $\lambda_u=5$, b - wing with smaller control surface located $0.05b_u$ below vortex axis with $\sigma=0.2$, $\alpha_0=2.5^\circ$, $\beta=2.5^\circ$, $\lambda_u=5$, c - wing in vortex axis with $\alpha=0^\circ$; $\alpha_0=2.5^\circ$, $\beta=2.5^\circ$, $\sigma=0.3$, $\lambda_u=5$.

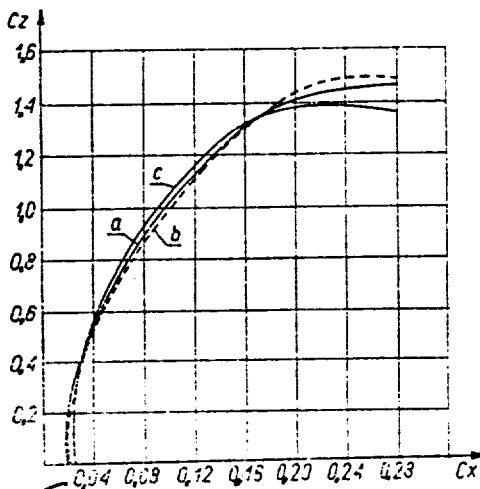


Figure 11. Effect of control surface aspect ratio λ_u on wing curve characteristics with $\alpha_0 = 2.5^\circ$, $\beta = 2.5^\circ$, $\sigma = 0.3$, $\lambda_w = 5$;
a-comparative wing with λ_w equal to 5
b-wing with λ_u equal to 7
c-wing with λ_u equal to 3

Increasing the aspect ratio of the control surface λ_u from 5 to 7 did not produce any marked differences in curves except for an insignificant increase in $C_{z_{max}}$ as shown in Fig. 11. Analysis of this result permits the opinion that increasing the control surface aspect ratio decreased the interaction of the exterior part of the horseshoe vortex and, despite smaller stream deflection angles, the disadvantageous effects of the control surface did not change practically. Advantageous effects of increasing the aspect ratio of the control surface appear only with a simultaneous enlargement of the span or aspect ratio of the wing in order to preserve the same physical wing proportions of negative and positive stream deflection angles. To test this idea, a

$(\lambda_u = 3.0)$

wing curve was calculated for a control surface aspect ratio of λ . In fact, in the central part of the curve a better shape was realized though at the expense of decreasing Cz_{max} as well as increasing Cx_{min} . In this regard, a tandem arrangement with control surface and wing of equal spans will present the least advantage (because of the smaller increment of ΔCz for the wing in comparison to the control surface, which makes it impossible to simultaneously attain Cz_{max} for both surfaces). It is necessary to add here that coefficient $\frac{\partial Cz}{\partial \lambda}$ for the control surface grows as its aspect ratio increases which is not a requirement with regard to longitudinal stability. The influence of changing the control surface aspect ratio on the wing curve (having the same span and aspect ratio) is shown in Figure 11.

5. Comparison of a canard with a twisted wing with a conventional arrangement

Although in a canard arrangement, the control surface plays an important role in creating lift, comparison of characteristics of just wings of canard and conventional arrangements is not decisive. For this reason, curves were also recalculated for both arrangements being compared considering a control surface with a deflected flap. The conventional arrangement consisted of the same untwisted wing and a control surface with a JA 177 profile and aspect ratio of $\lambda = 3.35$.

With regard for the need to apply vertical force on the bottom of a conventional control surface, which is related to the deflection of the flap, and the need to attain Cz_{max} , its magnitude was taken as 4 percent ^{of} ~~to~~ the lift on the wing (average value obtained from several aircraft). For the canard arrangement, the same magnitude of vertical force on top was also taken as 4 percent of lift on the wing and added to the control surface relative to flap deflection necessary to attain Cz_{max} for the wing.

Comparing both curves presented in Figure 12, it is seen that for the canard case an increase of about 40 percent in the lift coefficient Cz_{\max} is attained as opposed to the conventional arrangement though at the expense of increasing Cx_{\min} by about 80 percent. Choosing a canard arrangement, therefore, is advantageous in cases where largest lift coefficient Cz_{\max} for an arrangement is a deciding factor in the aircraft's construction concept.

Presented in Figure 13 is a comparison of graphs of $Cz/Cx = f(\alpha)$ characterizing the lift to drag ratio which makes further comparison of the two arrangements possible. The conventional arrangement always possesses a maximal relation of Cz to Cx , larger than for the canard. In fact, after adding in a value for harmful drag of Cx_{harm} equal to 0.03, the differences diminish quite distinctly though the conventional arrangement continues to be better with respect to lift to drag ratio for the whole range of angles of attack. Thus the canard takes a second place to the conventional arrangement with regard to properties of distance flight or the aircraft's angle of glide.

Another factor in arrangements given as $Cz^3/Cx^2 = f(Cz)$ is equally advantageous to the conventional arrangement if only the wing and control surface are compared, though the curve characterizing the canard is flatter and a large value of coefficient Cz^3/Cx^2 is spread out over a larger range of Cz values than in the case of a conventional arrangement (Figure 14). The situation changes when the harmful drag is added to the coefficients of drag for these arrangements since the relationship $(Cz^3/Cx^2)_{\max}$ occurs for the canard arrangement for greater angles of attack and for greater values of coefficient Cz . A canard might appear more advantageous when subjected to certain magnitudes of harmful drag though through smaller magnitudes of harmful drag the usually applied wing-control surface arrangement is undoubtedly better.

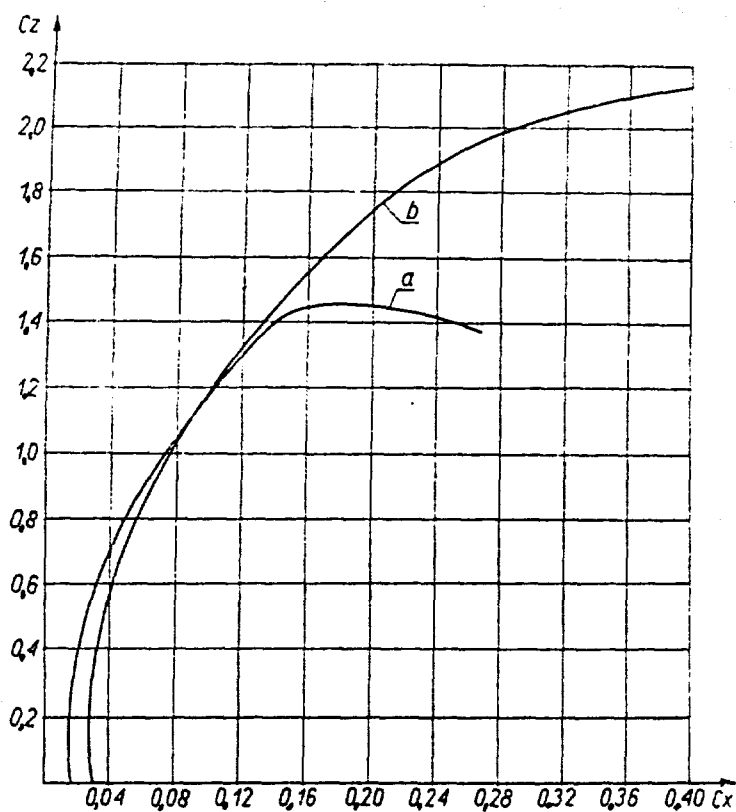


Figure 12. Comparison of curves for canard and conventional arrangements.
 a-conventional arrangement
 b-canard arrangement

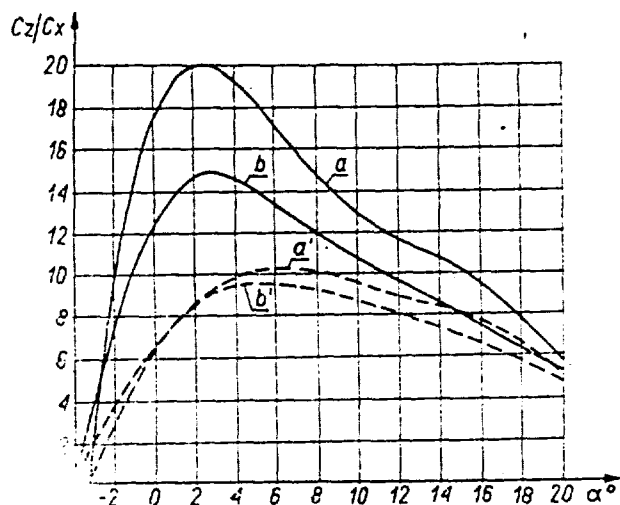


Figure 13. Comparison of curves for canard and conventional arrangements.
 a, a'-conventional arrangement
 b, b'-canard arrangement
 a', b'-taking harmful drag into account

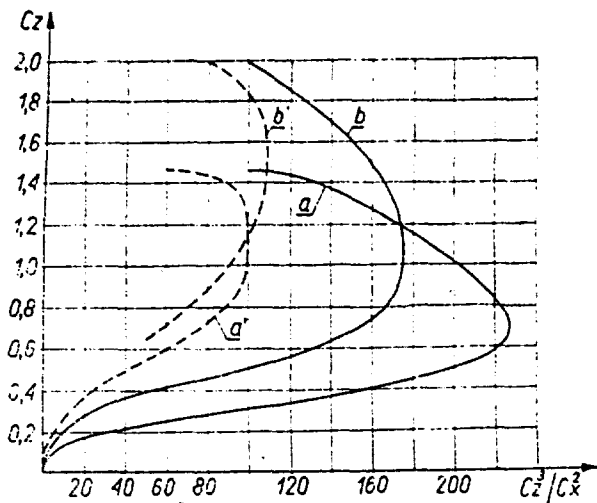


Figure 14. Comparison of the function $C_z^3/C_x^2 = f(C_z)$ for canard and conventional arrangements.
 a, a'-conventional arrangement
 b, b'-canard arrangement
 a', b'-taking into account harmful drag

In the foregoing case, for harmful drag coefficients of $C_{x_{szk}}$ equal to 0.03, $(C_z^3/C_x^2)_{max}$ attained a slightly smaller value for the conventional versus the canard arrangement.

6. The problem of the shift of the center of upthrust

In order to ascertain the shift of the center of upthrust for a canard arrangement, the location of the resultant aerodynamic forces was recalculated as a function of the angle of attack for the same arrangement. This was required to assess the effect of the probable relocation of the center of force of the canard.

The relocations were performed with the assumption that the aerodynamic forces on the wing and control surface were located along the aerodynamic axes of each lift surface (wing and control surface) at 25 percent of the distance between the chord and the edge of incidence. The calculation did not include the respective movement of the center of upthrust of each surface individually during changes in angle of attack but took into account only the relocation of the resultant aerodynamic forces resulting from the chosen canard arrangement.

It is necessary to note that the effect of stream deflection on the relocation of the resultant aerodynamic forces is disadvan-

tageous relative to longitudinal stability. In fact, coefficient $\frac{\partial C_z}{\partial x}$ is smaller for the control surface with respect to its smaller aspect ratio but the stream deflection past the control surface in the region between the horseshoe vortex axes decreases $\frac{\partial C_z}{\partial x}$ of this portion of the wing so effectively that for the observed case the average coefficient $\frac{\partial C_z}{\partial x}$ for the entire wing is smaller than for the control surface even though the parts of the wing lying outside the vortex have $\frac{\partial C_z}{\partial x}$ greater than for the wing in undisturbed flow. This effect was discussed in greater detail in part 2.

As can be seen from the curves in Fig. 15, the shift of the center of upthrust is equally dependent on the angle of setting β of the control surface. This shift is particularly marked when the angle of attack changes between 0 and 5 degrees (C_z changes in value from 0.413 to 0.937) and amounts to 6 percent of the wing chord for β equal to 2.5 degrees.

For a control surface angle setting β equal to 5 degrees, the shift of the center of upthrust for α between 0 and 5 degrees (C_z changes in value from 0.508 to 0.997) amounts to 17.5 percent of the wing chord.

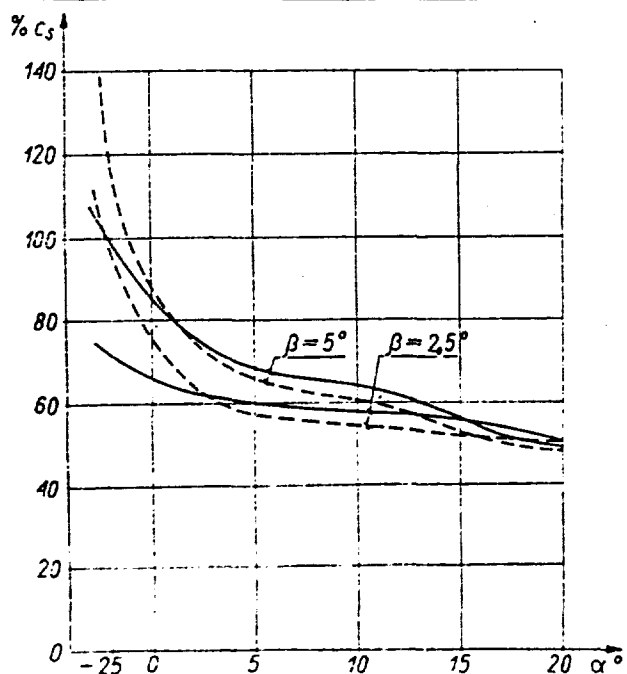


Figure 15. Location of the center of upthrust of a canard as a function of the angle of attack for $\sigma=0.3$, $\alpha_0=2.5^\circ$, $\lambda_u=5$, $\lambda_s=7$;
 -distance given as a percentage of wing chord distance in direction forward of wing's aerodynamic axis,
 -distance between the aerodynamic axes of the wing and control surface amounts to $3.4 c_u$
 -dashed lines signify the changes which occur in the location of

the center of upthrust in a canard arrangement given the condition that there are no stream deflections past the control surface

Corresponding values for the case if the flow past the control surface was undisturbed would amount to 18 percent of the wing chord for β equal to 2.5 degrees during a change in angle of attack of 0 to 5 degrees, while for β equal to 5 degrees the shift amounts to 23 percent of the wing chord. These values were calculated for the given distance of $3.4 c_u$ between the aerodynamic axes of the wing and control surface. These values increase with an increase of this distance.

7. Conclusions

Summing up the gained results and the current discernment of the problem of a canard arrangement, one can formulate the following conclusions;

1. Utilizing a frontal, horizontal control surface in a canard aircraft increases the total lift of a wing-control surface combination by a value equal to close to the relation between the horizontal control surface and the wing. An advantage can be therefore gained in reducing the constructed weight by taking more rational advantage of the control surface thereby increasing the usable weight of the aircraft. This matter has a deciding influence on the economics of using those aircraft that stop and start often and do not fly long distances.
2. The relation of C_z to C_x is worse for a canard than for an analogous conventional arrangement with the exception of the case of the untwisted wing for smaller angles of attack. In this case, however, smaller values of the coefficient $C_{z_{max}}$ are obtained. The canard arrangement does not lend itself to aircraft of long range or large gliding flight angles for purely economic dictates. In this regard, a canard is less preferable to a conventional aircraft.

3. The relation of $(C_z^3/C_x^2)_{max}$ for the same combination of wing-control surface is worse in the case of a canard than a conventional arrangement but if one looks at the whole aircraft, this situation could be reversed. For aircraft for which it is impossible to gain large aerodynamic lift to drag ratios for reason of their purpose, a relatively large magnitude of harmful drag acts to the advantage of a canard, also a greater value of the relation $(C_z^3/C_x^2)_{max}$ can be obtained than for the conventional arrangement. From this one can conclude that both the speed of ascent as well as a minimal force needed to stay airborne can be more advantageously gained for a canard in the case when it is impossible for the entire aircraft to be aerodynamically pure. This is important in the cases of simple transportation or agricultural aircraft or for those of similar purposes.

4. Relative to the small drag coefficient $C_{x_{min}}$ for the untwisted wing, given smaller angles of attack, a canard can be more advantageous for a high speed aircraft equipped with appropriate wing devices for gaining high values of lift coefficient $C_{z_{max}}$. In association with the probable large shift in the aerodynamic center in the transonic speed range, a canard is also a good solution for a fast aircraft.

5. Utilization of a frontal control surface is equally more advantageous during take off and landing relative to ground effects. While for a canard, ground effects help in attaining a greater lift on the horizontal control surface, in a conventional arrangement the effect is negative although for an aircraft to move through a large angle of attack and gain $C_{z_{max}}$ it is necessary to deflect the elevators more to attain an appropriate magnitude of lift on the bottom of the control surface.

6. The presented material enables an orientation of where to look for the optimal solution for aircraft arrangements with frontal control surfaces. All the possibilities were not investigated to their conclusion and the problems of longitudinal and side stability were not addressed though these require separate

treatment.

Work submitted to the editor's office in February 1975

SOURCE DOCUMENTS

1. *Spreiter J. R. and Sacks A.*: Trailing vortex sheet effect on downwash, J.A.S. January 1951.
2. *Silverstein A., Katzow A. and Bullivant W. A.*: Downwash and wake behind plain and flapped airfoils, NACA, Rep. 651, 1939.
3. *Ostoslawski J. W.*: Aerodynamika samoleta. Oborongiz, Moskwa. 1957.
4. *Gates S. B.*: Notes on the tail-first aeroplane, R.M. 2676, July 1939.

DISTRIBUTION LIST

DISTRIBUTION DIRECT TO RECIPIENT

<u>ORGANIZATION</u>	<u>MICROFICHE</u>	<u>ORGANIZATION</u>	<u>MICROFICHE</u>
A205 DMATC	1	E053 AF/INAKA	1
A210 DMAAC	2	E017 AF/RDXTR-W	1
B344 DIA/RDS-3C	9	E403 AFSC/INA	1
C043 USAMIIA	1	E404 AEDC	1
C509 BALLISTIC RES LABS	1	E408 AFWL	1
C510 AIR MOBILITY R&D LAB/FIO	1	E410 ADTC	1
C513 PICATINNY ARSENAL	1	FTD	
C535 AVIATION SYS COMD	1	CCN	1
C591 FSTC	5	ASD/FTD/NIIS	3
C619 MIA REDSTONE	1	NIA/PHS	1
D008 NISC	1	NIIS	2
H300 USAICE (USAREUR)	1		
P005 DOE	1		
P050 CIA/CRB/ADG/SD	2		
NAVORDSTA (50L)	1		
NASA/NST-44	1		
AFIT/LD	1		
LLL/Code L-389	1		
NSA/1213/TDL	2		